Prestack depth imaging of multi-azimuth seismic data in the presence of orthorhombic anisotropy

Yi Xie
CGGVERITAS
Singapore
yi.xie@cggveritas.com

Sergey Birdus
CGGVERITAS
Perth, Australia
sergey.birdus@cggveritas.com

James Sun
CGGVERITAS
Singapore
james.sun@cggveritas.com

Carl Notfors
CGGVERITAS
Singapore
carl.notfors@cggveritas.com

SUMMARY

The presence of orthorhombic anisotropy can severely affect the imaging of multi- and wide- azimuth data which is rapidly developing with the benefit of better illumination, better imaging, and better multiple elimination. Analysis of multi-azimuth (MAZ) data often reveals noticeable fluctuations in moveout between different acquisition directions, preventing constructive summation of MAZ images. Vertical transverse isotropy (VTI) effects can also co-exist causing well misties and higher order moveout. We have developed an approach for imaging in the presence of orthorhombic anisotropy. In this paper, we first describe our approach, including a newly developed orthorhombic imaging method and a newly developed practical method for orthorhombic anisotropy model building. We then demonstrate with both synthetic and real data from offshore Australia that our approach can successfully take into account the co-existing HTI/VTI effects, reduce the structural discrepancies between seismic images built for different azimuths, thereby producing constructive summation of MAZ datasets and resolving well misties to match with geology. The combined effect of these improvements is a step-change in the final seismic image quality.

Key words: Orthorhombic; Anisotropy; Multi-azimuth; Prestack depth migration.

INTRODUCTION

Orthorhombic anisotropy is considered to be the simplest realistic symmetry for many geophysical problems (Tsvankin, 1997a). Orthorhombic anisotropy exhibits both HTI (Horizontal Transverse Anisotropy) and VTI (Vertical Transverse Anisotropy) effects, making seismic velocity varying with azimuthal direction as well as polar direction. In many cases, these effects are important by themselves and can be a target of special studies.

The presence of orthorhombic anisotropy poses challenges in wide azimuth imaging. Analysis of multi-azimuth (MAZ) data often reveals noticeable fluctuations in moveout between different acquisition directions, preventing constructive summation of MAZ images (Dickinson et al 2010). VTI effects can also cause well misties and higher order moveout. Orthorhombic anisotropy takes into account the co-existing HTI/VTI effects. Thus, orthorhombic anisotropic PSDM can reduce the structural discrepancies between seismic images built for different azimuths, producing a constructive summation of MAZ dataset and resolving well misties.

In the following, we first describe our approach for imaging in the presence of orthorhombic anisotropy. Our orthorhombic PSDM approach is based on Tsvankin's work on anisotropy parameters and *P*-wave velocity for orthorhombic anisotropy. We develop our ray tracing method suitable for both weak and strong anisotropy, which applies to both Kirchhoff and Beam PSDM (Notfors *et al*, 2006). In order to demonstrate the ability of our method to perform multi-azimuth imaging in the presence of orthorhombic anisotropy, we apply our method to a 3D multi-azimuth data set acquired offshore Australia, which exhibits both azimuthal anisotropy and vertical transverse isotropy. By using our orthorhombic PSDM approach, we managed to account for both HTI and VTI effects present in the field seismic data.

METHOD AND RESULTS

Tsvankin (1997a) introduced the notation for orthorhombic anisotropy along the lines of Thomsen's parameters for VTI media. A typical orthorhombic symmetry model is shown as Figure 1 (Tsvankin, 1997a). The vertical symmetry planes are defined by the directions parallel and normal to the cracks. For *P*-wave imaging, the required parameters for an orthorhombic model include: V_{P_0}, the vertical velocity of the *P*-wave; ε_2, δ_2, anisotropy parameters in the symmetry plane $x_1 - x_3$, normal to symmetry axis x_2; ε_1, δ_1, anisotropy parameters in the symmetry plane $x_2 - x_3$, normal to symmetry axis x_1; δ_3, the VTI parameter of plane $x_1 - x_2$, where x_1 plays the role of the symmetry axis, and φ_2 is the azimuth angle of symmetry x_1. Following Tsvankin's work, we propose to compute the phase velocity in the following form, which removes the weak anisotropy restriction:

$$\frac{V^2(\theta,\phi)}{V_{P_0}^2} = \frac{1}{2}\left(1 + 2\varepsilon(\phi)\sin^2\theta + \sqrt{(1+2\varepsilon(\phi)\sin^2\theta)^2 - 8(\varepsilon(\phi)-\delta(\phi))\sin^2\theta\cos^2\theta}\right)$$
$$\varepsilon(\phi) = \varepsilon_1\sin^4\phi + \varepsilon_2\cos^4\phi + (2\varepsilon_2 + \delta_3)\sin^2\phi\cos^2\phi$$
$$\delta(\phi) = \delta_1\sin^2\phi + \delta_2\cos^2\phi \qquad (1)$$

where $V(\theta,\phi)$ is the phase velocity with θ as ray polar angle, ϕ as the azimuth angle of ray relative to symmetry axis x_1. Equation (1) gives an azimuth angle and polar angle

dependent phase velocity. Under acoustic approximation for orthorhombic media, we define the eikonal G as

$$G = \frac{1}{2}((1+2\varepsilon(\phi))(p_x^2+p_y^2)+p_z^2 + \sqrt{((1+2\varepsilon(\phi))(p_x^2+p_y^2)+p_z^2)^2 - 8(\varepsilon(\phi)-\delta(\phi))(p_x^2+p_y^2)p_z^2}) \equiv 1 \quad (2)$$

where p_x, p_y, p_z are the normalized slowness components (Zhou *et al*, 2003, Huang *et al*, 2007)

$p_x = \mathrm{p}_x / v_{p_0}$, $\quad p_y = \mathrm{p}_y / v_{p_0}$, $\quad p_z = \mathrm{p}_z / v_{p_0}$.

The eikonal G can be further derived as

$$G = 0.5\left(A + \sqrt{A^2 - 8\left((\varepsilon_1-\delta_1)p_y^2 + \frac{(\varepsilon_2+\delta_3)p_x^2 - \varepsilon_1 p_y^2}{p_y^2+p_x^2}p_x^2 + (\varepsilon_2-\delta_2)p_x^2\right)p_z^2}\right) \equiv 1$$

Where $A = (1+2\varepsilon_2)p_x^2 + (1+2\varepsilon_1)p_y^2 + p_z^2 + 2\frac{(\varepsilon_2+\delta_3)p_x^2 - \varepsilon_1 p_y^2}{p_y^2+p_x^2}p_x^2$

By defining the Hamiltonian $H(x,p) = V_{p_0}^2(x)(G-1)/4$, we build the orthorhombic ray tracing system, which honours both azimuthal angle and polar angle dependency of wave propagation. The ray tracing system can be used for both Kirchhoff and Beam PSDM.

Multi- and wide azimuth surveys provide the velocity information along different azimuths. Hung *et al* (2006) and Wombell (2006) describe how to estimate azimuthal anisotropy parameters for conventional narrow azimuth marine streamer data. Moreover, with vertical check shot surveys, vertical velocity at well locations can be accurately obtained. By making use of linear slip theory (Schoenberg *et al*, 1997, Bakulin *et al*, 2000), the effective anisotropy parameters of an orthorhombic model can be related to the set of HTI parameters and the set of VTI parameters as follows:

1. The symmetry plane $x_2 - x_3$, orthogonal to the HTI symmetry axis x_1, is purely VTI, solely determined by the estimated set of VTI parameters,
$$\varepsilon_1 = \varepsilon_{VTI}, \quad \delta_1 = \delta_{VTI}, \quad (3)$$
2. In the symmetry plane $x_1 - x_3$ orthogonal to the HTI symmetry axis x_2, we have
$$\varepsilon_2 = \varepsilon_{VTI} + \varepsilon_{HTI}^v, \quad \delta_2 = \delta_{VTI} + \delta_{HTI}^v, \quad (4)$$

where ε_{HTI}^v and δ_{HTI}^v are related to the conventional rotated Thomsen's parameters ε_{HTI} and δ_{HTI} as following (Tsvankin, 1997b),

$$\varepsilon_{HTI}^v = -\varepsilon_{HTI}/(1+2\varepsilon_{HTI})$$
$$\delta_{HTI}^v = (\delta_{HTI} - 2\varepsilon_{HTI}(1+\varepsilon_{HTI}))/(1+2\varepsilon_{HTI})^2 \quad (5)$$

The HTI parameters take into account and correct for the azimuthally dependent velocity variation. The VTI parameters provide the measure for slowing down the apparent velocity to match with geology and correct for the higher order moveout when necessary.

Examples

The first example compares the impulse responses of isotropic, VTI, HTI and orthorhombic PSDM respectively. Input impulse sits at inline 101, crossline 101. Table 1 lists the properties of the medium. In both HTI and orthorhombic cases, the azimuth angle of the slowest velocity direction (normal to fracture) is along the inline direction. Figure 2 compares the migrated sections of inline 101. It clearly shows that the presence of HTI causes azimuthally dependent wave propagation; VTI causes a polar angle dependent wave propagation, making events shallower for this case with $\delta \neq 0$. Orthorhombic effects cause both azimuthally and polar dependency of wave propagation. In the plane along the crossline direction, orthorhombic PSDM produces the same result as that by VTI PSDM as VTI is the only anisotropy in this plane. The plane along inline direction is determined by the combination of both HTI and VTI effects. This shows that by introducing orthorhombic anisotropy, we can account for both azimuthally dependent and polar dependent wave propagation. In this synthetic test, it images reflectors at shallower depths and makes velocity azimuthally dependent.

Orthorhombic PSDM was applied to a real dual azimuth 3D seismic dataset that had been acquired in an area of the North-West Australian shelf with known strong horizontal velocity anisotropy. As expected, the data were affected by both horizontal azimuthal and VTI velocity anisotropy. Figure 4 shows the initial isotropic PSDM gather and moveout at the same common reflection point, but of different surveys (with 35 and 89 degree acquisition azimuths respectively). The azimuthally dependent variation of residual moveout clearly shows the presence of azimuthal anisotropy. Figure 5 shows the gather and moveout by HTI PSDM. By taking into account HTI, azimuthally dependent residual moveout was taken care of, but the gather still has weak non-hyperbolic residual moveout, indicating the presence of VTI anisotropy. An orthorhombic velocity model was then built based on the estimated HTI and VTI models. Figure 6 shows the orthorhombic PSDM results. Orthorhombic modeling and imaging takes into account the co-located VTI and HTI effects, further flattens the gathers of both surveys, makes events shallower as expected. Figure 7 compares the gamma (residual velocity analysis) map from initial isotropic PSDM and orthorhombic imaging. Orthorhombic imaging effectively flattens the gathers of different azimuth surveys as well as non-hyperbolic moveout due to VTI (warmer color: more residual moveout, cooler color: less residual moveout).

Conclusions

We have developed and demonstrated an effective method for P-wave imaging in the presence of orthorhombic anisotropy. Synthetic and real data results show that our method can be used to effectively take into account both azimuthally and polar angle dependent wave propagation, which is of particular importance for multi- and wide azimuth surveys which have large azimuth coverage for a better constructive stack of image migrated from different azimuth survey and for better tie with well. Extending this work to orthorhombic systems tilted relative to the horizontal direction (the orthorhombic analog of tilted transverse isotropy) is straightforward.

References

Bakulin, A., Grechka, V., and Tsvankin, I., 2000, Estimation of fracture parameters from reflection seismic data - Part II:

Fractured models with orthorhombic symmetry: Geophysics, 65, 1803-1817

Dickinson, D., Ridsdill-Smith, T., 2010, Benefits of Multi-azimuth Depth Migration over the Tidepole Field, North West Shelf, Australia: 72nd Annual International Coference and Exhibition, EAGE, Extended Abstracts, B044.

Huang, T., Xu, S., and Zhang, Y., 2007, Anisotropic Estimation for Prestack Depth Imaging - A Tomographic Approach: 77th Annual International Meeting, SEG, Expanded Abstracts, 124-128.

Hung, B., Zhang F., Sun, J., Stanley, M., and Osadchuk, A., 2006, An Automated 3D Method for Azimuthal Anisotropy Analysis in Marine Seismic Data, 68th Annual International Coference and Exhibition, EAGE, Extended Abstracts, H035.

Notfors, C., Xie, Y., and Gray, S., 2006, Gaussian Beam Migration: A Viable Alternative to Kirchhoff?: 68th Annual International Coference and Exhibition, EAGE, Extended Abstracts, G046.

Schoenberg, M., Helbig, K., 1997, Orthorhombic media: Modeling elastic wave behavior in a vertically fractured earth: Geophysics, **62**, 1954–1974.

Tsvankin, I., 1997a, Anisotropic parameters and *P*-wave velocity for orthorhombic media, Geophysics 62, 1292-1309.

Tsvankin, I., 1997b, Reflection moveout and parameter estimation for horizontal transverse isotropy, Geophysics 62, 614-629.

Wombell, R., 2006, Characteristics of azimuthal anisotropy in narrow-azimuth marine streamer data, 68th Annual International Coference and Exhibition, EAGE, Extended Abstracts.

Zhou, H., Pham, D., Gray, S., and Wang, B., 2003, 3-D tomography analysis in TTI media: 73rd Annual International Meeting, SEG, Expanded Abstracts, 650-653.

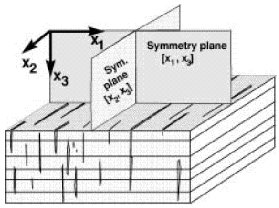

Figure 1 An orthorhombic model caused by parallel vertical cracks embedded in a medium composed of thin horizontal layers. Orthorhombic media have three mutually orthogonal planes of minor symmetry. From Tsvankin 1997a.

Table 1 Medium property for impulse response tests

Medium	v_{p_0} **m/s**	**Anisotropy parameters using Thomsen and Tsvankin's notation**
Isotropic	2000	NIL
VTI	1825	$\varepsilon_1 = \delta_1 = 0.1$
HTI	1690	$\varepsilon_1 = \delta_1 = 0.2, \theta = \pi/2, \phi = 0$
Orthorhombic	2000	$\varepsilon_1 = \delta_1 = 0.1, \varepsilon_2 = \delta_2 = -0.043, \delta_3 = 0.2, \phi_2 = 0$

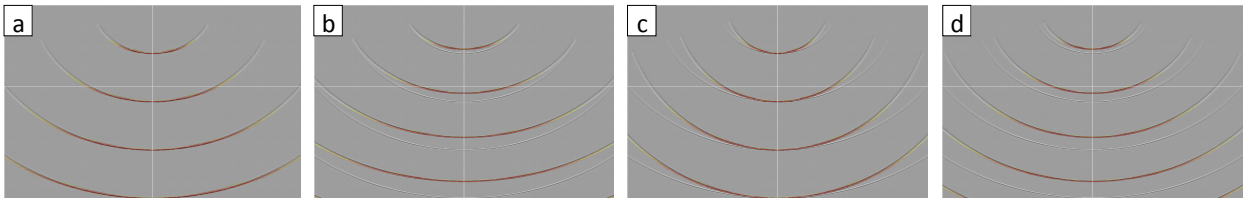

Figure 2 Inline 101 of impulse responses (in color) by a) isotropic PSDM, b) VTI PSDM, c) HTI PSDM, and d) orthorhombic PSDM, all overlain with isotropic PSDM result (in grey), in depth domain.

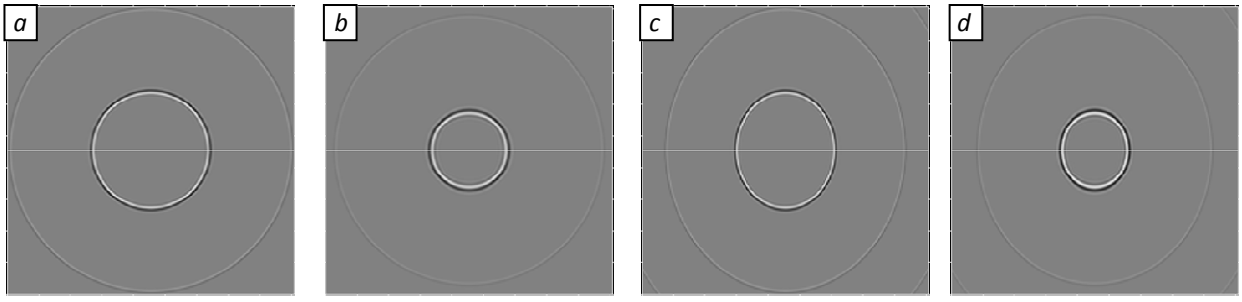

Figure 3 Depth slice of impulse responses by a) isotropic PSDM, b) VTI PSDM, c) HTI PSDM, and d) orthorhombic PSDM.

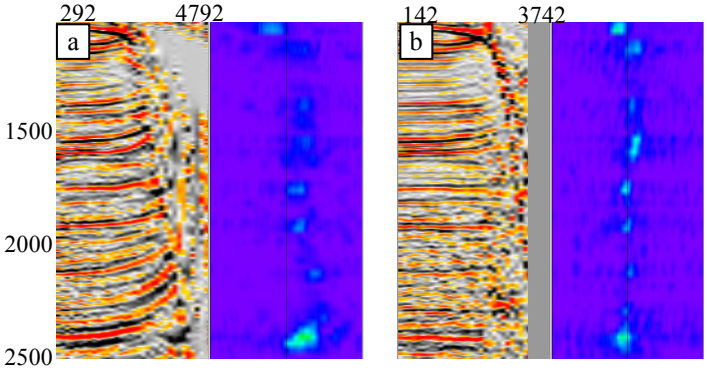

Figure 4 Isotropic PSDM, gather and semblance display of the same CRP location. a) survey with 89 degree acquisition azimuth, b) survey with 35 degree acquisition survey. HTI effect can clearly be seen.

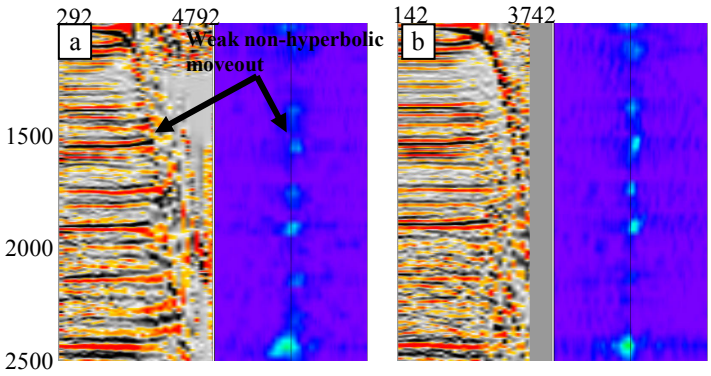

Figure 5 HTI PSDM, gather and semblance display of the same CRP location. a) survey with 89 degree acquisition azimuth, b) survey with 35 degree acquisition azimuth. Weak non-hyperbolic residual moveout indicates the existence of VTI

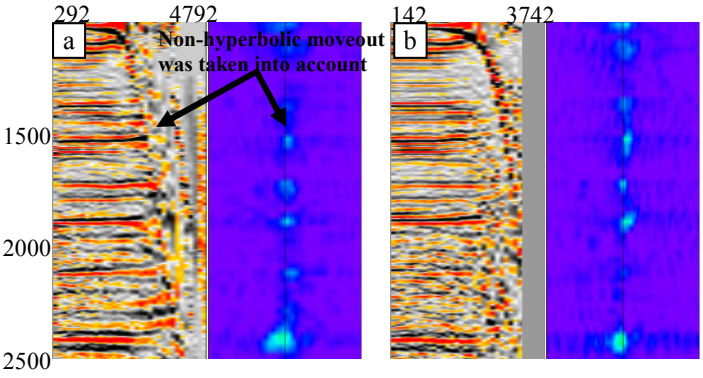

Figure 6 Orthorhombic PSDM, gather and semblance display of the same CRP location. a) survey with 89 degree acquisition azimuth, b) survey with 35 degree acquisition azimuth. Takes into account collocated HTI and VTI effects.

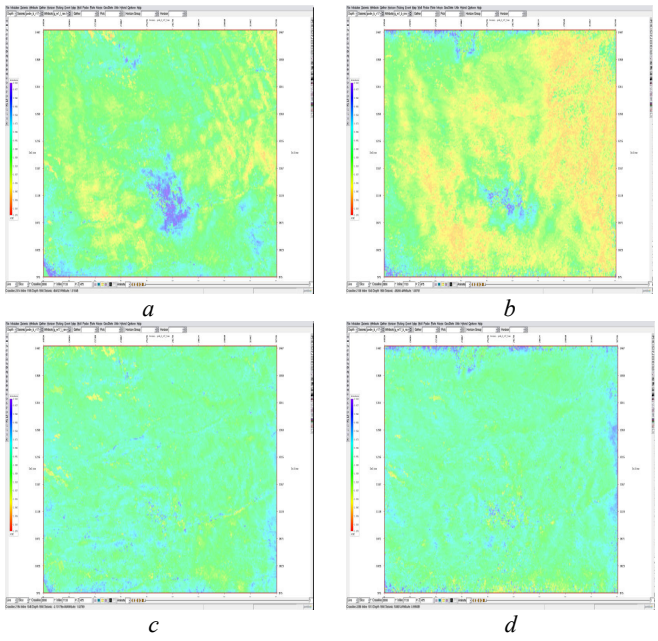

Figure 7 Gamma map at depth 1900m. a) Isotropic PSDM, survey with 89 degree acquisition azimuth; b) Isotropic PSDM, survey with 35 degree acquisition azimuth; c) Orthorhombic PSDM, survey with 89 degree acquisition azimuth; d) Orthorhombic PSDM, survey with 35 degree acquisition azimuth. Gamma volume measures the residual moveout. Warm color: more residual moveout, cool color: less residual moveout.